6 Chloride-Induced Corrosion Durability of High-Performance Fiber-Reinforced Cementitious Composites

State-of-the-Art Review

Shaikh Faiz Uddin Ahmed, Hirozo Mihashi, and Tomoya Nishiwaki

CONTENTS

6.1 INTRODUCTION

High-performance fiber-reinforced cementitious composites (HPFRCCs) are short fiber (either metallic and/or polymeric)-reinforced cement-based composites that exhibit strain-hardening and multiple-cracking behaviors in uniaxial tension and bending (Figure 6.1) (Naaman and Reinhardt 2006). Engineered cementitious composite (ECC) is the most significant development in the field of HPFRCC. ECC was originally developed at the University of Michigan (Li 1992). It typically exhibits tensile strain capacity of more than 3%, with spacing between multiple cracks at saturation less than 3 mm and maximum crack width less than 100 μm. Microstructure optimization allows ECC to be made with fiber content less than 2% by volume.

Ductile fiber-reinforced cementitious composites (DFRCCs) are another class of HPFRCCs that exhibit multiple-cracking behavior in bending (Ahmed et al. 2006; Kawamata et al. 2003). The Japan Concrete Institute (JCI) committee on DFRCC defined it as "cementitious composite materials reinforced with short fibers, which exhibit multiple-cracking characteristics under bending stress" (JCI-DFRCC Committee 2003). Both ECC and DFRCC are HPFRCC and drew attention of researchers and professionals due to their strain-hardening and multiple-cracking behavior in

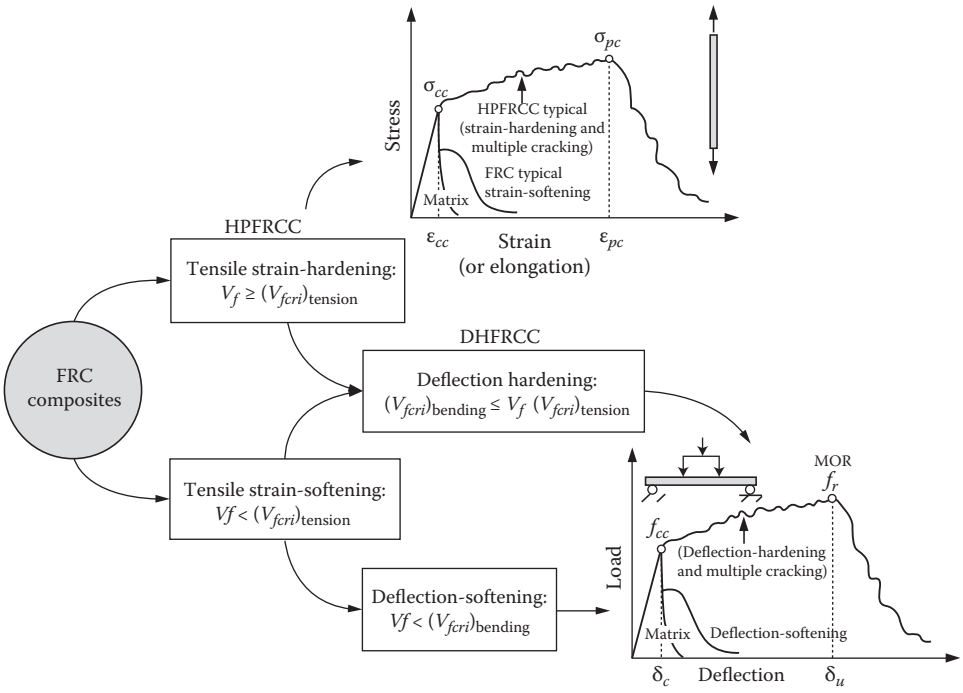

FIGURE 6.1 Classification of FRC and HPFRCC composite. (From Naaman, A.E. and Reinhardt, H.W., *Materials and Structures*, 39: 547–555, 2006. With permission.)

tension and/or bending. ECCs exhibit superior crack width and spacing control in the pseudo strain-hardening phase. Typical strain hardening and multiple cracking of ECC and DFRCC in uniaxial tension and bending are shown in Figures 6.2 and 6.3, respectively. ECC with such superior tensile response can be engineered by tailoring the composite ingredients with the aid of micromechanically based formulations (Li and Wu 1992; Li and Leung 1992), which result in multiple finely spaced cracks of controlled widths. This crack control may be exploited for its potential inherent

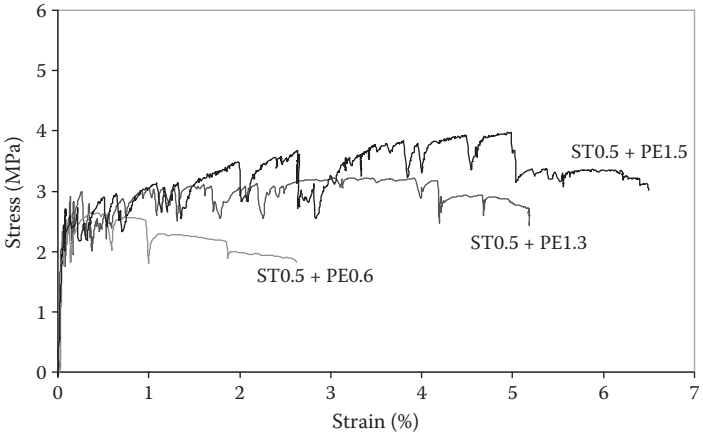

FIGURE 6.2 Typical example of strain-hardening and multiple-cracking behavior of ECC in uniaxial tension. (From Ahmed, S.F.U. et al., *ASCE, Journal of Materials in Civil Engineering*, 19(7): 527–539, 2007. With permission.)

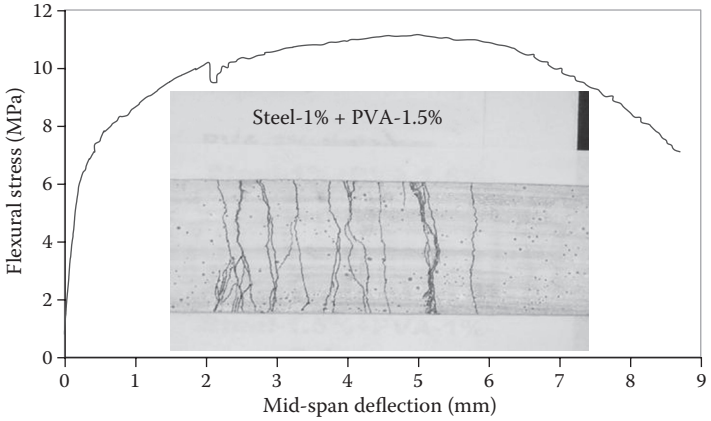

FIGURE 6.3 Typical example of multiple-cracking behavior of DFRCC under four-point bending. (From Ahmed, S.F.U. et al., *Journal of Construction and Building Materials*, 21: 1088–1097, 2006. With permission.)

durability and the durability it may afford to the reinforced concrete (RC) structures that are deteriorating rapidly (e.g., corrosion damage).

It has been demonstrated that for corrosion durability, the use of more than one type of fiber as reinforcement will result in a *hybrid-fiber composite* that is better able to meet the material performance requirements (Ahmed et al. 2006, 2007). For instance, to use HPFRCC in corrosion-resistant structures, a low crack width is required to reduce the ingress of aggressive substances reaching the steel reinforcement, while at the same time, a high strain capacity is also required to prevent delamination and concrete cover spalling. Further, given that mono fiber HPFRCCs containing high-modulus fibers (e.g., steel and carbon fibers) normally exhibit high ultimate strength, low crack width, and low strain capacity, while those containing low-modulus fibers (e.g., polyvinyl alcohol [PVA] and polyethylene [PE] fibers) exhibit opposite behaviors, it becomes clear that a hybrid-fiber HPFRCC with a proper volume ratio of high- and low-modulus fibers can be designed to achieve an optimal balance between ultimate strength, crack width, and strain capacity (Figure 6.4) and, therefore, better meet the functional requirement for corrosion durability application.

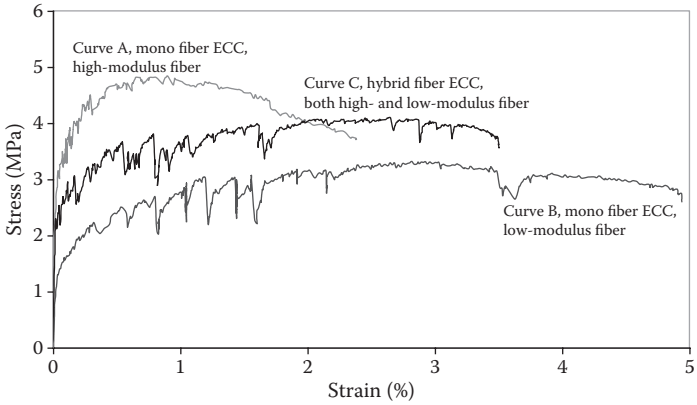

FIGURE 6.4 Concept of hybrid reinforcement in HPFRCC, where simultaneous improvement of strength, strain/ductility, and crack width can be observed. (From Ahmed, S.F.U. et al., *ASCE, Journal of Materials in Civil Engineering*, 19(7): 527–539, 2007. With permission.)

6.2 CORROSION DURABILITY CHARACTERISTICS OF HPFRCC

This section will discuss some of the most essential properties of HPFRCC that directly influence the corrosion of steel.

6.2.1 Tight Crack Width Properties

The durability of RC structures can be enhanced by controlling the width of cracks, because these cracks, if wide enough, provide access to the deteriorating agents to reach the reinforcements in the RC structures and easily cause corrosion of reinforcing steels. Load and environmentally induced cracks are inherent in RC structures and are difficult to control. The crack width in RC flexural members scales with the square root of concrete cover thickness (Gergely and Lutz 1973). Therefore, the width of exposed cracks increases as the cover thickness increases. Attempts to reduce the crack width by reducing the concrete cover thickness will lead to much worse corrosion, as it becomes easier for corrosive substances to penetrate and reach the reinforcement through the smaller cover of concrete material. Various design codes limit the crack width in RC structures for corrosion protection. A summary is given in the work of Ahmed and Mihashi (2007). The crack width limits for an aggressive environment are so low that it is generally difficult to achieve in practice using commonly used reinforcing steel and conventional concrete due to incompatible tensile deformation of concrete with steel in RC as shown in Figure 6.5a, whereas in the case of reinforced HPFRCC, numerous multiple cracks of narrow width are formed due to its strain-hardening behavior and compatible tensile deformation with steel (Figure 6.5b). Due to the strain-hardening and multiple-cracking behavior of HPFRCC, it is argued that the cracks that formed are of narrow width and will satisfy the crack width limit for durability imposed by the design codes. Control of crack width using HPFRCC has been demonstrated by several researchers. The earliest report of crack width measurement is by Maalej and Li (1995), where PE fiber-reinforced ECC is used to replace the part of the concrete that surrounds the main flexural reinforcement in an RC beam, and it is shown that the maximum crack width in the beam under service load can be limited to values that are very difficult to achieve using conventional steel reinforcement and commonly used concrete. In their study, the average crack width under service load in the ECC layer at the bottom of the beam was found to be 0.10 mm (Figure 6.6). Average crack width of about 0.060 mm in ECC containing PVA fibers in uniaxial tension is reported by Li et al. (2001). Another study that included crack width measurements was conducted by Ahmed and Mihashi (2010), where maximum crack width of 0.06 and 0.09 mm are reported in reinforced HPFRCC beams containing hybrid steel and

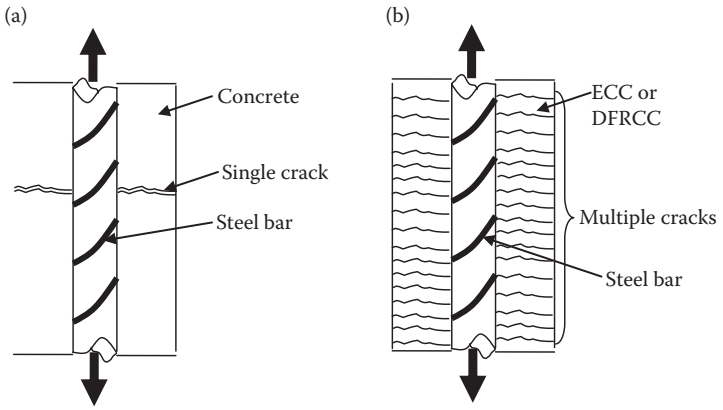

FIGURE 6.5 Incompatible tensile deformation in R/C (a) versus compatible tensile deformation in R/ECC or R/DFRCC (b) through ductile, multiple-cracking tensile response of ECC or DFRCC.

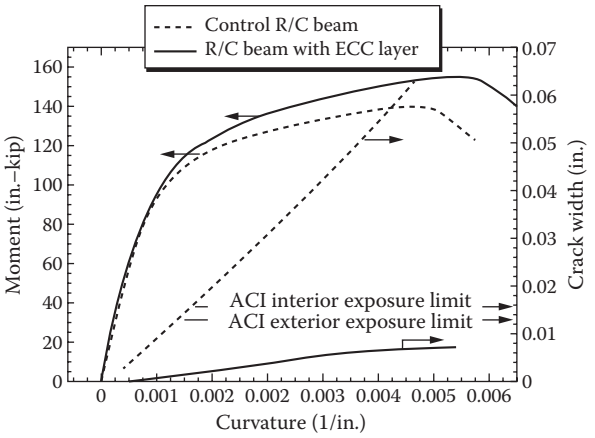

FIGURE 6.6 Crack width of RC beam and RC beam with ECC layer under flexural loading. (After Maalej, M. and Li, V.C., *ACI Structural Journal*, 92(2): 167–176, 1995. With permission.)

PE fibers (Figure 6.7), respectively, when both beams were subjected to about 80% of their corresponding calculated ultimate load in bending. The above results clearly show that the cracks thus formed in the HPFRCC under service load are small enough to resist the penetration of aggressive substances into the concrete and that the durability of RC structures can be enhanced greatly using this material.

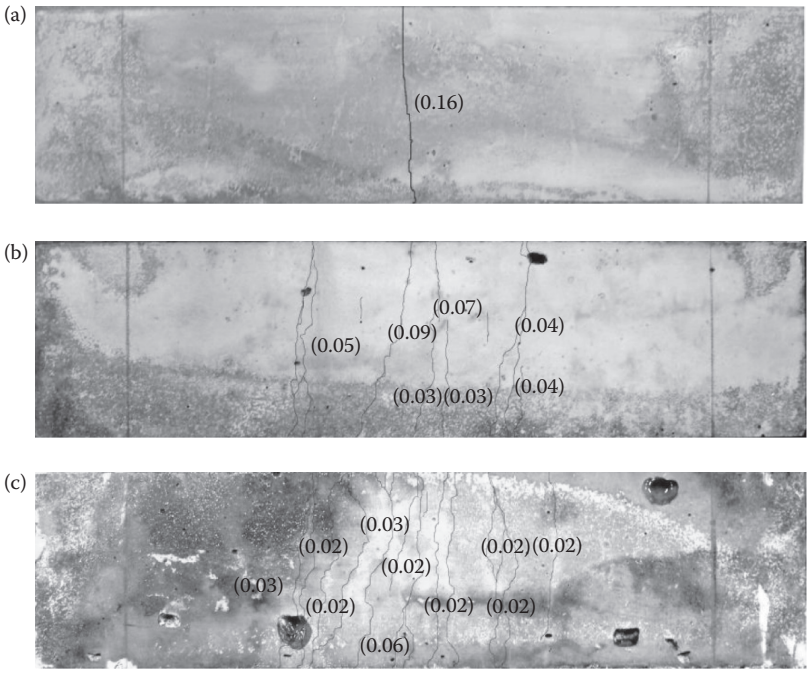

FIGURE 6.7 Cracking pattern on the tension face of the specimens after four-point bending with a maximum load of about 80% of their corresponding calculated ultimate load (crack widths in millimeters are presented in the parentheses). (a) Beam containing ordinary mortar. (b) Beam containing PE fiber-reinforced SHFRCC material. (c) Beam containing hybrid steel-PE fiber-reinforced SHFRCC material. (From Ahmed, S.F.U. and Mihashi, H., *Australian Journal of Civil Engineering*, 8(1): 13–25, 2010. With permission.)

6.2.2 Permeability Characteristics of Cracked HPFRCC

Transport properties of concrete, especially permeability, affect the durability and integrity of a structure. High permeability, due to porosity or cracking, provides ingress for water, chlorides, and other corrosive agents. If such agents reach reinforcing bars within the structure, the bars corrode, thus compromising the ability of the structure to withstand loads, which eventually leads to structural failure. Although most of the design codes recommend limits for allowable maximum crack width in the RC as a function of exposure conditions, the limits for aggressive environments are unrealistic when considering costs and available resources of conventional practice of ordinary RC. Although cracking in concrete structures cannot be completely avoided, more effective means to control cracking in the RC members must be attempted in order to prevent excessive permeability.

6.2.2.1 Water Permeability of Cracked HPFRCC

Since the permeability significantly influences the deterioration of concrete, evaluation of water permeability in cracked HPFRCC seems a key factor to describe the durability performance of given materials. Superior impermeability of HPFRCC has been observed by several researchers. Lepech and Li (2005) studied the water permeability of cracked HPFRCC and reinforced mortar specimens. When subjected to identical tensile deformation, the HPFRCC and reinforced mortar specimens exhibited very different cracking patterns and widths. They found that the cracked HPFRCC exhibits nearly the same permeability as sound concrete, even when strained in tension to several percent (Figure 6.8). Homma et al. (2009) also evaluated the water permeability of cracked

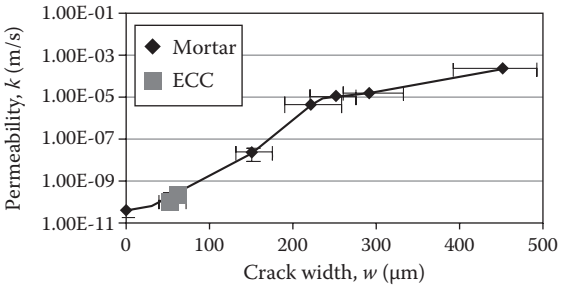

FIGURE 6.8 Water permeability as a function of crack width of cement-based composite materials. (After Lepech, M. and Li, V.C., Durability and long term performance of engineered cementitious composites, *Proceedings of the International Workshop on HPFRCC in Structural Applications*, Honolulu, Hawaii, May 23–26, 2005. With permission.)

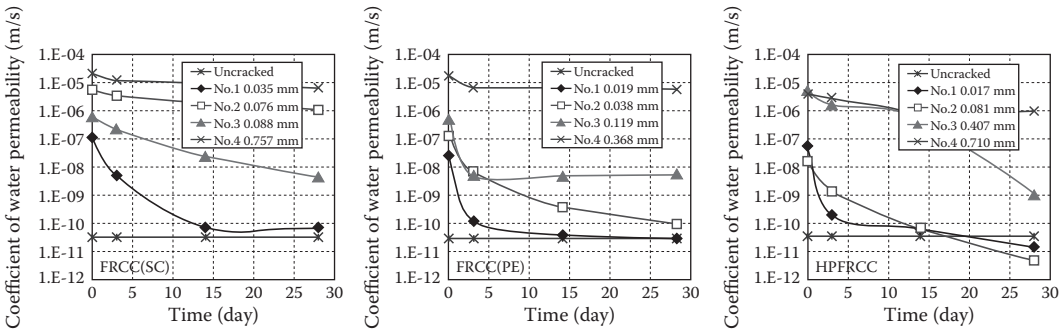

FIGURE 6.9 Comparison of water permeability of uncracked and cracked HPFRCCs having different crack widths. [Note: FRCC(SC) and FRCC(PE) are HPFRCCs containing steel and PE fiber, respectively. HPFRCC is steel–PE fiber-reinforced HPFRCC.] (From Homma, D. et al., *Journal of Advanced Concrete Technology*, 7(2): 217–228 2009. With permission.)

HPFRCC materials. They also reported comparable water impermeability of cracked HPFRCC to that of uncracked specimen (Figure 6.9). They have also reported the formation of healing products in the cracks in HPFRCC, which contributed to the better water permeability resistance that will be discussed in the next section.

In another study, Martinola et al. (2002) evaluated the water permeability of cracked and uncracked HPFRCC by water absorption test. In their study, the amount of water taken up by capillary suction was determined on cubes cut out from the middle section of the beams, which were subjected to a four-point bending test. Maximum crack width in the cracked HPFRCC specimens was found to be about 0.10 mm. Both cracked and uncracked HPFRCC exhibited very low water absorption coefficient in their study.

6.2.2.2 Chloride Permeability/Penetration of Cracked HPFRCC

While the penetration of water into the concrete contributes to the onset of corrosion of steel, the penetration of chlorides and other chemical substances accelerate the corrosion process. No systematic study of permeability and penetration of chloride as a function of crack width has been performed to date for HPFRCC. However, comparative tests on steel-reinforced concrete or mortar beams (R/C or R/mortar) and steel-reinforced HPFRCC (R/HPFRCC) beams have been performed by a limited number of researchers (Maalej et al. 2003; Miyazato and Hiraishi 2005; Ogawa et al. 2005; Kobayashi et al. 2010). Maalej et al. (2003) studied the chloride penetration in medium-scale R/C and R/HPFRCC beams measuring 300 × 210 × 2500 mm. In their study, both R/C and R/HPFRCC beams were preloaded in three cycles of loading and unloading up to 70% of their estimated ultimate load in order to create flexural cracks in the beams prior to an accelerated corrosion test. The crack widths in unloaded condition were 0.2 and 0.12 mm in R/C and R/HPFRCC beams, respectively. In the corrosion test, the bottom half of both beams were submerged in water containing 3% NaCl (by weight) and were subjected to cyclic wetting and drying for about 3 months. At the end of the corrosion test, chloride content in concrete and HPFRCC at the level of reinforcing steels was measured by collecting powder samples at the bottom of the beams. The results showed that the chloride content in the HPFRCC beams was much lower (about four times lower) than that of the RC beam. Miyazato and Hiraishi (2005) also studied the depth of chloride penetration in small-scale R/mortar and R/HPFRCC beams. Beams with a cross-section of 100 × 100 mm, reinforced by a single reinforcing bar placed centrally and with a 20-mm cover to the tensile surface, were subjected to three-point bending with a span of 350 mm. All beams were loaded to 20 kN, causing a single crack in the R/mortar beam with a width of 0.3–0.4 mm but several cracks in the R/HPFRCC beams with a width below 0.1 mm. These crack widths were maintained during the corrosion test. Both beams were subjected to accelerated chloride exposure conditions, with alternating wet and dry cycles for 28 days. During the wet cycle, the specimens were exposed to a saltwater shower (3.1% NaCl by weight) at 90% relative humidity (RH) for 2 days. During the dry cycle, the specimens were exposed to 60% RH for 5 days. The beams, after environmental exposure, were split, and a 0.1 mol/L $AgNO_3$ solution was sprayed onto the fractured surface after the steel bar was removed. The chloride penetration depth was determined at various locations along the beam, by measuring the depth from the tensile side of the beam surface to the boundary where the color was changed. In the case of the R/mortar beams, it was found that chloride penetration was approximately 80–100 mm. In the case of the R/HPFRCC beams, chloride penetration occurred at multiple locations corresponding to where the multiple cracks were formed during the preload. However, the penetration depth was much shallower than that found in R/mortar and distributed between 0 and 20 mm.

In another study, Ogawa et al. (2005) studied the chloride ion penetration resistance of beams made with ordinary concrete and HPFRCC. In their study, 8-mm-thick HPFRCC plates were cast. A 100 × 100 × 400 mm mold was built from the cut pieces of the 8-mm-thick HPFRCC plates. Ordinary concrete was poured into this mold. An ordinary concrete specimen of the same size was also prepared. Both specimens were cured under water for 38 days and were soaked in artificial seawater containing 1.8% chloride ion concentration for 30 and 60 days. Test results showed that

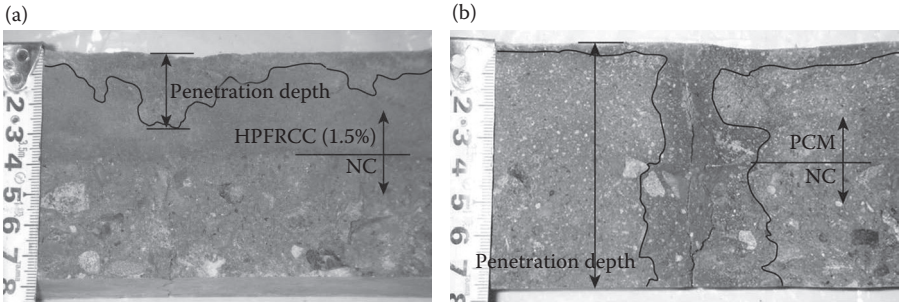

FIGURE 6.10 Chloride penetration profiles in beams containing HPFRCC repair layer (a) and polymer cement mortar (b). (After Kobayashi, K. et al. *Cement and Concrete Composites*, 32: 411–420. With permission.)

in the case of ordinary concrete specimens, the chloride ion concentration was about 0.04% after 60 days of soaking, whereas in the case of HPFRCC specimens, the chloride ion concentration was only 0.005%, about 10 times lower than that of ordinary concrete.

Recently, Kobayashi et al. (2010) also studied the chloride penetration into the cracked HPFRCC material. In their study, several concrete beams were prepared, and the bottom layer surrounding the reinforcing steel was repaired using HPFRCC and repair mortar (polymer cement mortar [PCM]). Cracks were introduced in the specimens by uniaxial tension. The maximum crack widths in the HPFRCC repair layer and PCM layer were 0.06 and 0.43 mm, respectively. The specimens were then subjected to saltwater (containing 3% NaCl) spray for 5 min every 6 h and continued for 2 months. Similar to Miyazato and Hiraishi (2005), the $AgNO_3$ solution was also sprayed on the fractured surface to measure the chloride penetration depth. Reduced chloride penetration in cracked HPFRCC compared to PCM was reported in their study (Figure 6.10). The above results on the permeability of HPFRCC show that it has very low water and chloride permeability even in the crack state.

6.3 SELF-HEALING CAPABILITY OF CRACKS IN HPFRCC

In addition to the low water and chloride permeability of cracked HPFRCC described above, the narrow width of these microcracks has the potential to promote self-healing. For example, Edvardsen (1999) showed that the dominant factors for promoting self-healing in concrete are a small crack width and the exposure condition. Research also suggests that water content and the presence of pozzolanic materials in concrete also facilitate the self-healing of cracks through further hydration of unhydrated cement in the cracks and through pozzolanic reaction. The first reported study on the self-healing of cracks in HPFRCC was reported by Homma et al. (2009). In their study, the self-healing of cracks is confirmed through tension and water permeability tests and the observation of self-healed products on the crack faces. The evidence of self-healed products in the crack surface can be seen in Figure 6.11, and the evidence of tensile strength recovery after the self-healing can be seen in Figure 6.12. Self-healing of cracks in HPFRCC is also confirmed by other researchers such as Yang et al. (2009) (Figure 6.13), Qian et al. (2009), Kan et al. (2010), Li and Li (2011), and Koda et al. (2011) (Figure 6.14). A brief summary of the types of HPFRCC with different crack widths used in the self-healing studies can be found in Table 6.1.

6.3.1 Corrosion Resistance of HPFRCC

Corrosion resistance of reinforcing steel in RC is essential for long-term durability of RC infrastructure. While the corrosion of reinforcing steel in ordinary concrete and even in high-performance

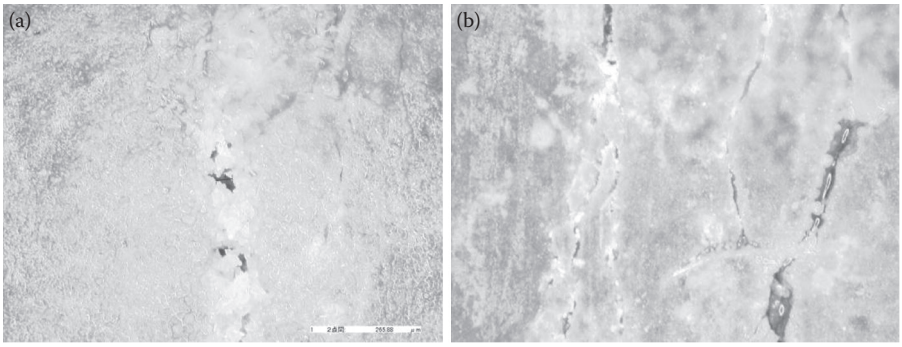

FIGURE 6.11 Evidence of self-healing of cracks in PE fiber-reinforced HPFRCC (a) and PE–steel fiber-reinforced HPFRCC (b). (From Homma, D. et al., *Journal of Advanced Concrete Technology*, 7(2): 217–228, 2009. With permission.)

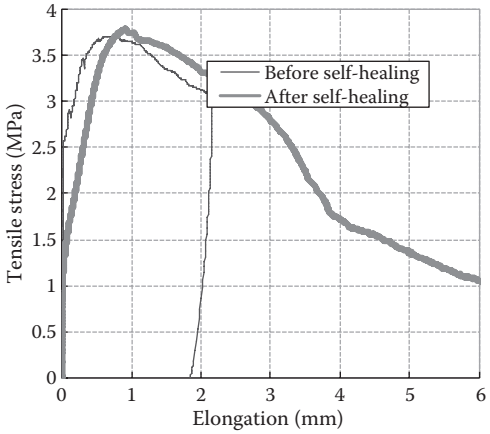

FIGURE 6.12 Recovery of tensile strength after self-healing of cracks in steel–PE fiber-reinforced HPFRCC. (From Homma, D. et al., *Journal of Advanced Concrete Technology*, 7(2): 217–228, 2009. With permission.)

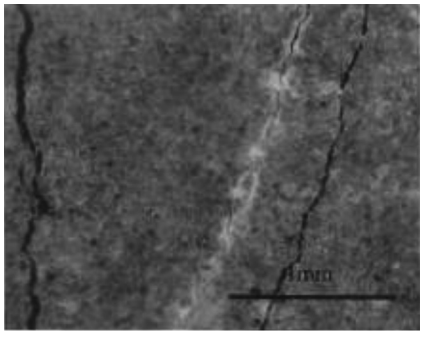

FIGURE 6.13 Self-healing of cracks in ECC. (From Yang, Y. et al., *Cement and Concrete Research*, 39: 382–390, 2009. With permission.)

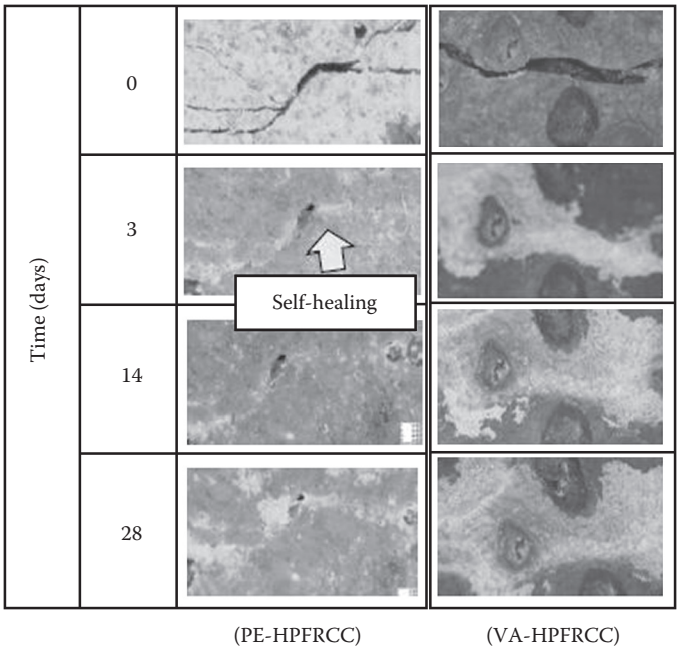

FIGURE 6.14 Self-healing of cracks in PE and PVA fiber-reinforced HPFRCC. (From Koda, M. et al., Self-healing capability of fiber reinforced cementitious composites, *Proceedings of the International Workshop on Advances in Construction Materials Through Science and Technology*, Hong Kong, RILEM Proceedings Pro 79, 2011. With permission.)

concrete has been researched extensively, the corrosion resistance of HPFRCC materials has been evaluated by a limited number of researchers. The first reported research was back in 1995, where Maalej and Li (1995) proposed a promising approach to address the problem of corrosion durability in RC structures using the ECC. Their study introduced a concept of functionally graded concrete (FGC) beams, in which the bottom layer of the beam including the part surrounding the main flexural reinforcement was cast with the ECC as discussed in the earlier section (Figure 6.15a).

Maalej et al. (2003) later adopted the above concept to prepare a series of FGC beams where a layer of DFRCC material exhibiting strain hardening and multiple cracking under third-point flexural loading is used around the main longitudinal reinforcement for corrosion protection (Figure 6.15b). The effectiveness of DFRCC material in retarding the corrosion of reinforcing steel in RC beams has been evaluated experimentally in this study. Two series of beams were tested in an accelerated corrosion environment. In the first series, a medium-scale RC beam measuring 300 × 210 × 2500 mm containing ordinary concrete was considered (Table 6.2). The second series was similar to the first series in every aspect except that the ordinary concrete that surrounded the main flexural steel reinforcement in the bottom was replaced with an optimized DFRCC made of hybrid fiber containing 1% steel and 1.5% PVA fibers. The beams in the second series were termed FGC beams. All beams in that study were precracked prior to undergoing accelerated corrosion. The precracking was achieved by subjecting the beams under four-point bending up to 70% of this estimated ultimate load. After unloading, the measured maximum crack widths in the specimens containing ordinary concrete and DFRCC layer were 0.2 and 0.13 mm, respectively. The accelerated corrosion in the beams was achieved by applying an 8-V fixed electrical potential to the anode (the main flexural reinforcement in the beams) and by subjecting the bottom half of the beams to cyclic wetting and drying cycles using water containing 3% NaCl. After the accelerated corrosion test, the RC beam containing ordinary concrete lost an estimated 10.1% of its steel reinforcement in about 83 days (Figure 6.5). During the same accelerated corrosion period, the

TABLE 6.1
Summary of Studies on Self-Healing of Cracks in HPFRCC

Reference	HPFRCC Types	Crack Width (mm)	Curing of Specimen before Self-Healing	Environmental Exposure Condition for Self-Healing	Water/ Binder	Presence of Pozzolans
Homma et al. (2009)	Steel fiber ECC (0.75% by vol.), PE fiber ECC (1.5% by vol.), Steel–PE–ECC (1.5% by vol.)	0.035 0.019 0.017	Air cured in lab for 1 week	Immersed in water tank at 20ºC for 28 days	0.45	15% silica fume
Yang et al. (2009)	ECC–PVA (2% by vol.)	0.06	Air cured in lab for 6 months	20 days of wet–dry cycles at 20ºC	0.25	55% fly ash (class F)
Qian et al. (2009)	PVA–ECC (2% by vol.)	0.06	Cured in sealed condition for 28 days at 20ºC	Immersed in water tank at 20ºC for 28 days Leave in air for 28 days	0.31–0.60	20% fly ash or slag
Kan et al. (2010)	PVA–ECC (2% by vol.)	0.08	Air cured in lab for 3 days and 3 months	Wet–dry cycles	0.27	55% fly ash (class F)
Li and Li (2011)	PVA–ECC (2% by vol.)	0.05	Air cured in lab for 28 days	Immersed in 3% NaCl solution for 30, 60, and 90 days	0.27	55% fly ash (class F)
Koda et al. (2011)	PVA–ECC (1.5% by vol.), PE–ECC (1.5% by vol.)	0.168 0.294	Water cured in lab for 28 days	Immersed in water tank at 20ºC for 91 days	0.45	15% silica fume

FGC beam specimen, FGC-2, lost an estimated 6.6% of its steel reinforcement. Specimen FGC-3 (the second FGC specimen), on the other hand, took about 141 days to reach the target 10% calculated steel loss. It was also observed that an FGC beam takes about 70% more time to achieve the same level of induced steel loss compared to an ordinary Portland cement concrete (OPCC) beam (Figure 6.16). The longer time required by specimen FGC-3 to reach the same level of calculated steel loss as ordinary concrete RC beam is probably due to the higher resistance of the DFRCC material to chloride ion penetration as well as the smaller width of the multiple cracks (or lower permeability) of DFRCC and the

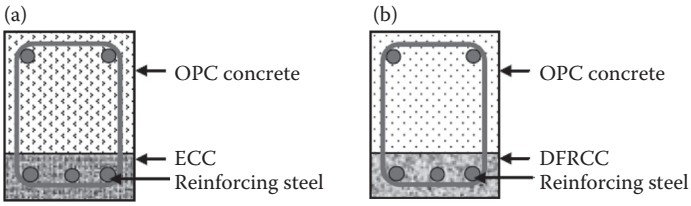

FIGURE 6.15 Concept of FGC: FGC containing ECC (a) (from Maalej, M. and Li, V.C., *ACI Structural Journal*, 92(2): 167–176, 1995) and FGC containing DFRCC (b) (from Maalej, M. et al., *Journal of Advanced Concrete Technology*, 1(3): 307–316, 2003. With permission from JCI.).

TABLE 6.2
Summary of Experimental Program

Series No.	Specimen Designation	Use of Special Layer	Structural Testing	FOSS Gauge	Accelerated Corrosion	Estimated Steel Loss
1	OPCC-1 (control)	Nil	Yes	No	No	—
	OPCC-2	Nil	Yes	Yes	Yes	10%
2	FGC-1 (control)	DFRCC	Yes	No	No	—
	FGC-2	DFRCC	Yes	Yes	Yes	6.6%
	FGC-3	DFRCC	Yes	Yes	Yes	10%

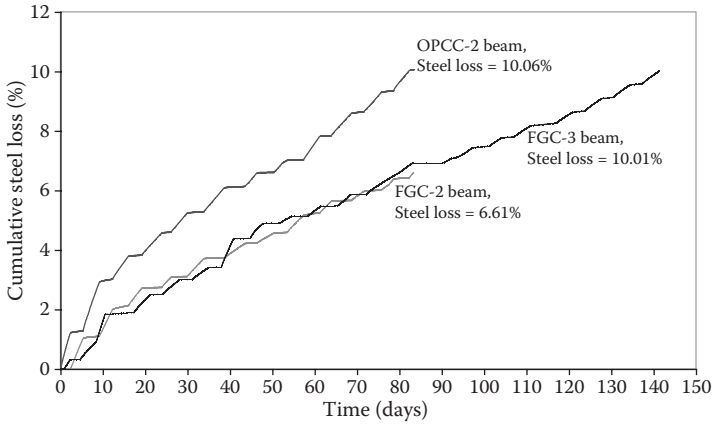

FIGURE 6.16 Steel loss of ordinary RC beam (OPCC-2 beam) and FGC beams in accelerated corrosion test. (From Maalej, M. et al., *Journal of Advanced Concrete Technology*, 1(3): 307–316, 2003. With permission from JCI.)

absence of corrosion-induced cracking in the FGC beams. The FGC beams exhibited a lower level of steel loss and longer time to achieve the same level of steel loss than an RC beam (Figure 6.17).

Recently, Ahmed and Mihashi (2010) have also evaluated the corrosion resistance of cracked beams made with mono and hybrid fiber-reinforced ECC materials and compared it with that of a plain mortar beam. The mono fiber ECC contained PE fiber of 1.5% by volume, while the hybrid-fiber ECC contained both steel and PE fibers of 0.75% each with a total fiber volume fraction of 1.5%. Small beam specimens 100 × 100 × 400 mm in dimension were used in their study. The beams were precracked under three-point bending with a maximum load of about 80% of their corresponding calculated ultimate load. Mono and hybrid ECC beams exhibited numerous multiple cracks with an average crack width of 0.05 and 0.026 mm, respectively, while the mortar beam exhibited a single crack 0.16 mm wide (Figure 6.7). Corrosion resistance of HPFRCC material was measured electrochemically using mini sensors placed on a reinforcing bar in each beam. Test results showed better corrosion resistance of ECC materials in terms of higher half-cell potential and polarization resistances values than that of ordinary mortar (Figures 6.18 and 6.19). The hybrid ECC beam also exhibited excellent corrosion-induced damage resistance compared to the mortar beam and the mono fiber ECC beam. It could be attributed to the better tensile strain-hardening characteristics of this material compared to mono ECC and mortar.

Superior corrosion resistance of HPFRCC material in a long-term durability study has also been reported by Mihashi et al. (2011b). This study is similar to the study reported by Ahmed and Mihashi (2010) in every aspect (such as the same ECC materials and similar beams), except the duration of the corrosion test and the measurement of corrosion of steel. In this study, the beams were subjected

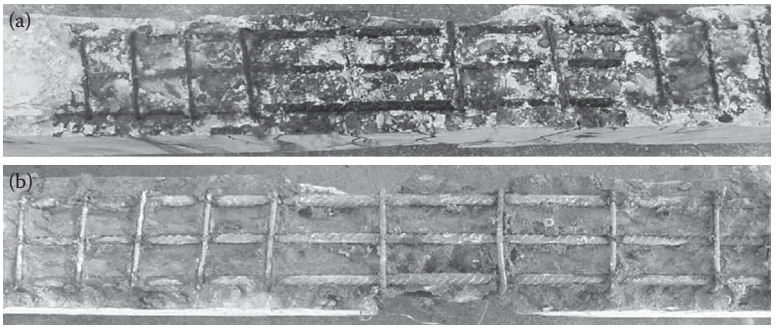

FIGURE 6.17 Corrosion status of steel in an OPCC-2 beam (a) and FGC-3 beam (b). (From Maalej, M. et al., *Journal of Advanced Concrete Technology*, 1(3): 307–316, 2003. With permission from JCI.)

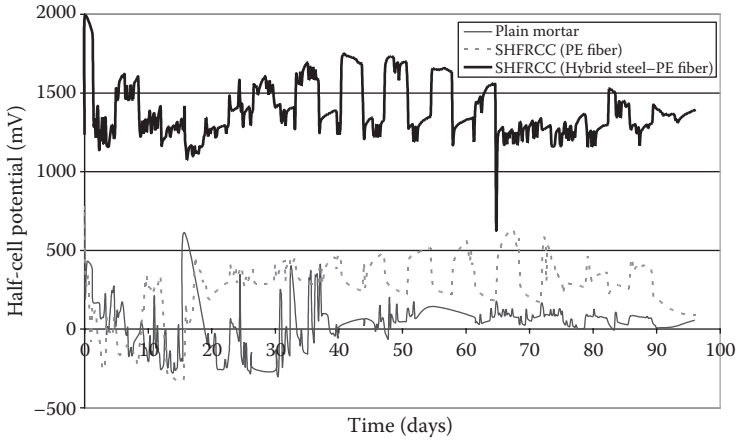

FIGURE 6.18 Measured half-cell potential values of beams with progress of time. (From Ahmed, S.F.U. and Mihashi, H., *Australian Journal of Civil Engineering*, 8(1): 13–25, 2010. With permission.)

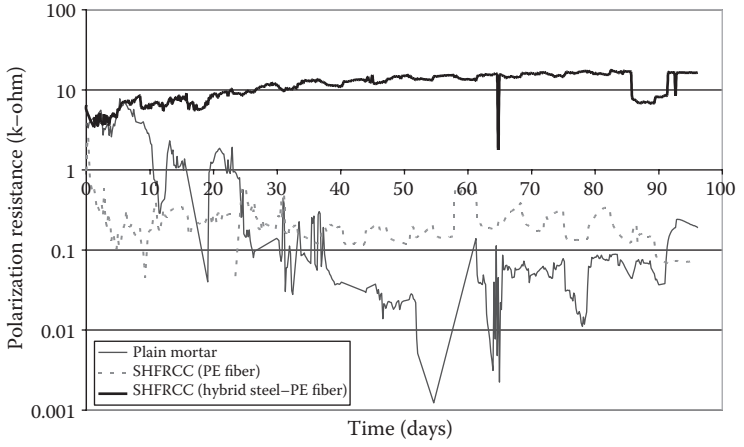

FIGURE 6.19 Measured polarization resistance values of beams with progress of time. (From Ahmed, S.F.U. and Mihashi, H., *Australian Journal of Civil Engineering*, 8(1): 13–25, 2010. With permission.)

to accelerated corrosion for 1 year, and the measured corrosion current was used to calculate the steel loss using Faraday's second law. Superior corrosion resistance of ECC beams in terms of lower steel loss (Figure 6.20) and very low corrosion-induced damage (Figure 6.21) was reported in this study.

In a study reported by Miyazato and Hiraishi (2005), two small-scale beams measuring 100 × 100 × 400 mm were subjected to accelerated chloride-induced corrosion. The first beam was an ordinary mortar beam, while the second beam contained DFRCC material containing 1.5% PVA fiber. In their study, bending cracks were also generated before subjecting the beams to accelerated corrosion. The crack width in the ordinary mortar beam was about 0.3–0.4 mm, while multiple cracks of width less than or equal to 0.1 mm were observed in the DFRCC beam. The accelerated corrosion in the beams was achieved by subjecting the beams to cyclic wetting (2 days) and drying (5 days) using water containing 3% NaCl for a period of 4 weeks. Negligible corrosion of steel in cracked DFRCC beams is observed compared to high macrocell and microcell corrosion at the location of cracks in a mortar beam in their study.

Sahmaran et al. (2005) also evaluated the corrosion resistance of ECC in an accelerated corrosive environment. Small prism specimens measuring 50 × 75 × 255 mm were used in their study. Better corrosion resistance of ECC over ordinary mortar was reported in their study. As can be seen from Figure 6.22, the current in the mortar specimens remained approximately 0.4 A until approximately 20 h, when a rapid increase in current was detected. The sudden rise in the current intensity coincided with the observation of a 0.3-mm crack width on the mortar specimens. The current recorded for the ECC specimens was much lower, at approximately 0.2 A until 15 to 20 h. The lower initial current recorded in the ECC specimens compared with the mortar specimens is due to

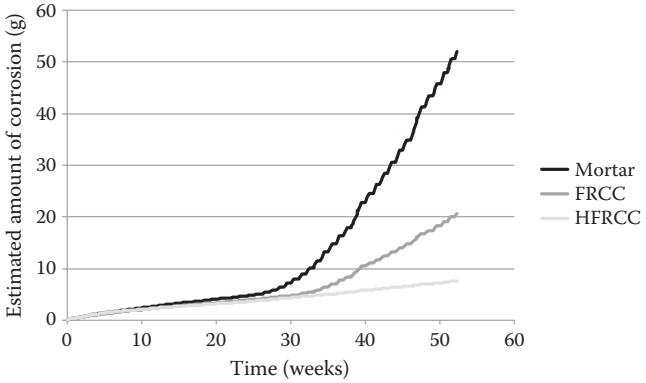

FIGURE 6.20 Amount of corrosion (estimated by Faraday's law) with progress of accelerated corrosion. (From Mihashi, H. et al., *Journal of Advanced Concrete Technology*, 9(2): 159–167, 2011. With permission.)

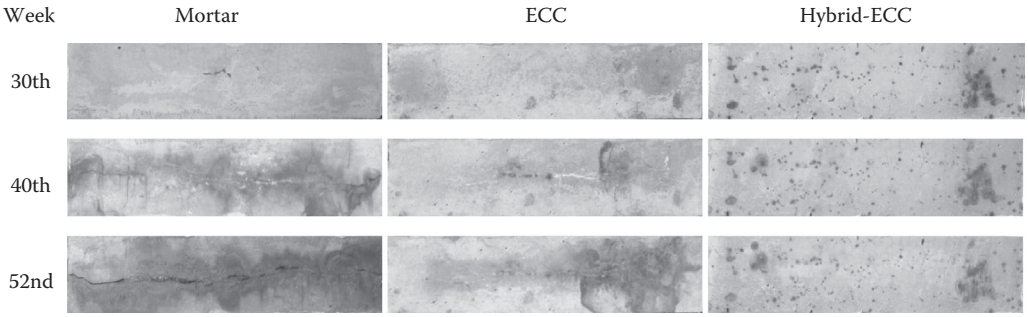

FIGURE 6.21 Time-dependent change of corrosion damage in the specimens made with plain mortar, ECC containing PE fiber, and steel–PE hybrid ECC. (From Mihashi, H. et al., *Journal of Advanced Concrete Technology*, 9(2): 159–167, 2011. With permission.)

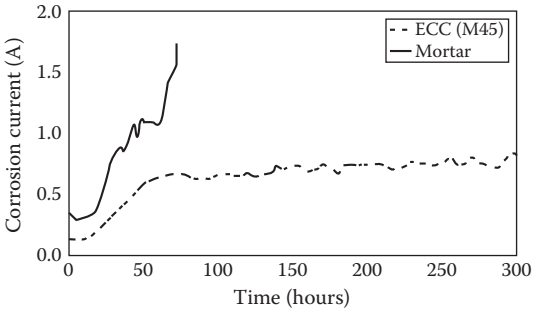

FIGURE 6.22 Corrosion of steel in mortar beam and ECC beam. (After Sahmaran, M. et al., *ACI Materials Journal*, 105(3): 243–250, 2008. With permission.)

the higher electrical resistivity of the ECC. The authors argued that this higher electrical resistivity of ECC is expected to be associated with a longer corrosion initiation period under field conditions.

6.3.2 Corrosion-Induced Damage Tolerance of HPFRCC

While HPFRCC exhibited superior protection of steel against corrosion in RC, only few studies evaluated its potential against corrosion-induced cracking and particularly against spalling/delamination of cover concrete in the RC beams. Due to their high fracture resistance and strain-hardening characteristics, the HPFRCC materials exhibit superior corrosion-induced damage tolerance compared with that of ordinary concrete.

In the study by Maalej et al. (2003), the corrosion-induced cracking was measured and monitored using a concrete embeddable fiber-optic strain sensor (FOSS) placed between the longitudinal bottom bars at the middle of each beam. The FOSS gauge was used to monitor the corrosion-induced tensile strain in the concrete at the level of longitudinal tensile reinforcement where splitting cracks are likely to occur (Figure 6.23). The better corrosion damage resistance of the FGC beams over the OPCC beam was also evident from the absence of any corrosion-induced cracks or damage and the lowest tendency for the concrete cover to delaminate as measured by a concrete embeddable FOSS. Figure 6.24 shows the variation of concrete strain as measured by the FOSS gauges over time in that study. During the first 27 days, the FOSS strain in the ordinary concrete specimen was slightly higher than those in FGC specimens (FGC-2 and FGC-3) and can be attributed to the higher rate of steel loss in the former beam compared to the latter ones. The measured strain in the ordinary concrete specimen increased with progress of corrosion, and the highest recorded FOSS reading was about 1686 microstrains. On the other hand, the rates of FOSS strain increase in both FGC specimens continued to be very low during the accelerated corrosion regime, and the highest recorded FOSS readings were 277 and 442 microstrains for specimens FGC-2 and FGC-3, respectively. Therefore, there was no

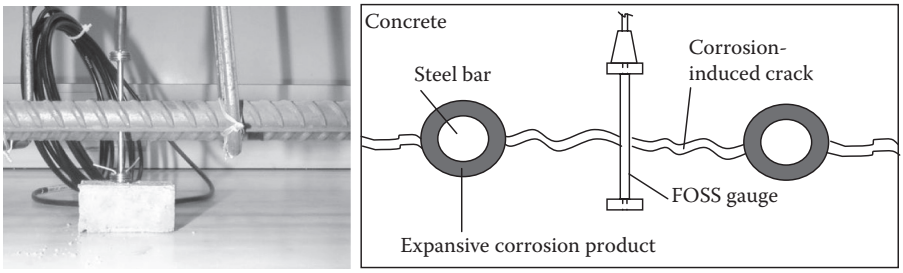

FIGURE 6.23 **(See color insert.)** FOSS gauge placed between longitudinal bottom bars (flexural reinforcements in beam) to measure and monitor the corrosion-induced tensile strain in concrete at the level of steel.

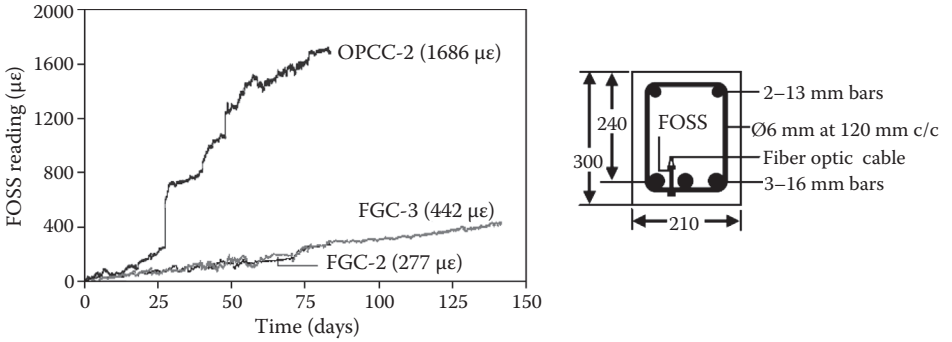

FIGURE 6.24 Corrosion-induced damage tolerance of OPC concrete and DFRCC material. (From Maalej, M. et al., *Journal of Advanced Concrete Technology*, 1(3): 307–316, 2003. With permission from JCI.)

sudden increase in FOSS strain recorded in the FGC specimens as there were no corrosion-induced cracks that had developed in either beam. The low FOSS readings and the absence of corrosion-induced cracks in the FGC specimens are probably due to the higher tensile strain capacity and fracture resistance of the DFRCC material compared to the ordinary concrete. The fibers in the DFRCC material suppress the growth of cracks and prevent strain localization, resulting in specimens that are free from corrosion-induced cracking. The FGC concept using the DFRCC material was found in the above study to be very effective in preventing corrosion-induced damage in RC beams and minimizing the loss in the beam's load and deflection capacities.

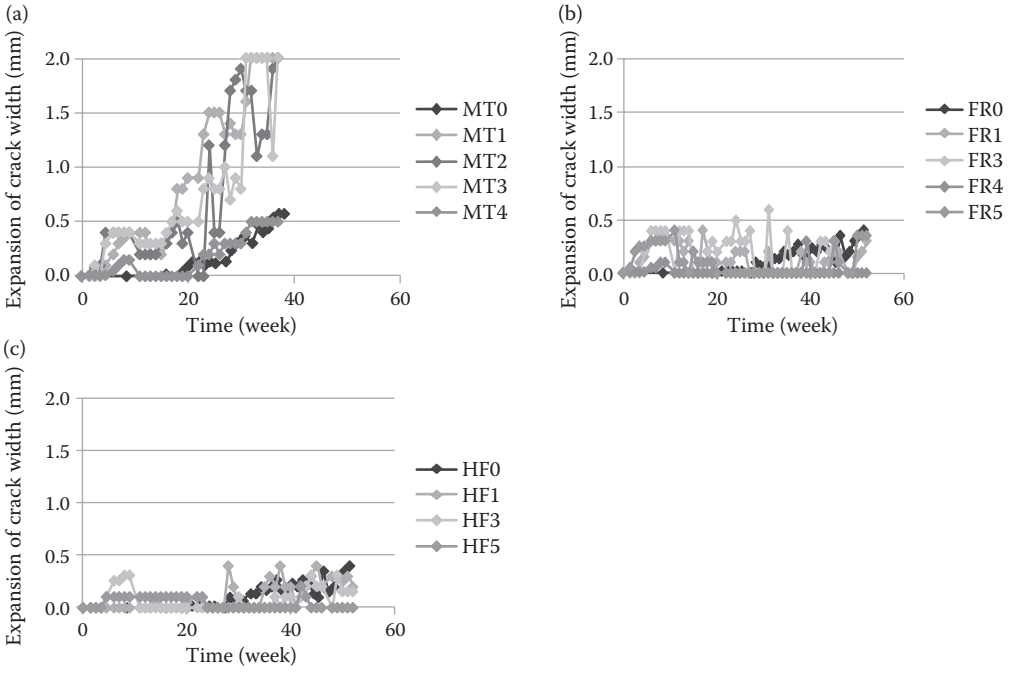

FIGURE 6.25 Change of the width of corrosion-induced longitudinal crack in the beams having different initially given crack widths in (a) mortar, (b) ECC containing PE fiber (represented as FR in the figure), and (c) ECC containing steel–PE hybrid fiber (represented as HR in the figure). (From Maalej, M. et al., *Journal of Advanced Concrete Technology*, 1(3): 307–316, 2003. With permission from JCI.)

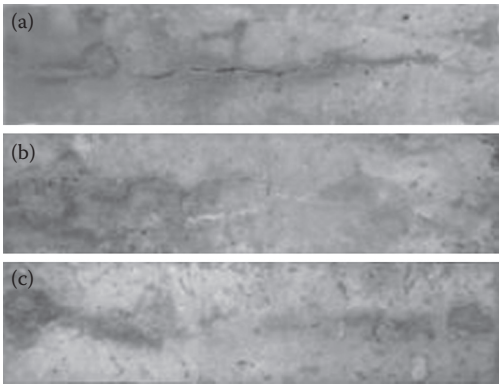

FIGURE 6.26 Typical corrosion-induced cracking in (a) mortar, (b) ECC containing PE fiber, and (c) ECC containing steel–PE hybrid-fiber beams. (From Mihashi, H. et al., Influence of crack widths on corrosion of reinforcing steel in fiber reinforced cementitious composites, *Proceedings of the International Workshop on Advances in Construction Materials Through Science and Technology*, Hong Kong, RILEM Proceedings Pro 79, 2011. With permission.)

Recently, Mihashi et al. (2011b) also monitored the corrosion-induced cracking of cracked ECC beams. The width of longitudinal cracks formed in the beams due to corrosion of steel was measured in ordinary mortar and ECC specimens during the accelerated corrosion test. The crack width of the mortar specimens increased with increase in corrosion exposure time. No such increase in the crack width in ECC specimens was observed in that study (Figure 6.25). This was also evident by comparing the corrosion-induced damage of ECC beams and mortar beam at any given time (see Figure 6.26).

6.3.3 Postcorrosion Structural Behavior of Corroded HPFRCC Beams

The postcorrosion structural responses of corroded RC beams containing ordinary concrete and HPFRCC materials have also been reported by few researchers. Maalej et al. (2003) evaluated the influence of DFRCC on the structural response of corroded FGC beams. Figure 6.27a shows the load–deflection curves of the corroded and uncorroded ordinary Portland cement (OPC) concrete beams. As the figure shows, the corroded beam (OPCC-2) lost about 13% of its ultimate load-carrying capacity and 9% of its deflection capacity at failure in comparison with those of the uncorroded one (OPCC-1). In the corroded specimen, after reaching the yield load, a longitudinal crack,

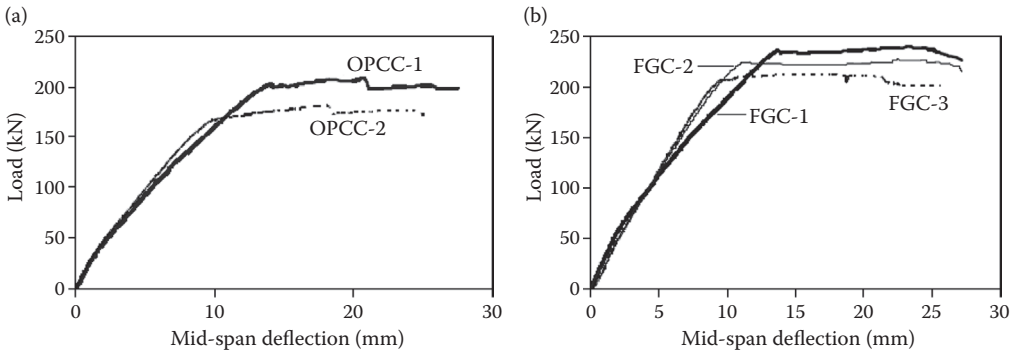

FIGURE 6.27 Load–deflection response of uncorroded and corroded beams: (a) OPCC beams and (b) FGC beams. (From Mihashi, H. et al., Influence of crack widths on corrosion of reinforcing steel in fiber reinforced cementitious composites. *Proceedings of the International Workshop on Advances in Construction Materials Through Science and Technology*, Hong Kong, RILEM Proceedings Pro 79, 2011. With permission.)

which had originally formed during the accelerated corrosion test, continued to increase in width as the load continued to increase. That led to slight delamination of the concrete cover upon reaching the peak load and cover spalling at failure as shown in Figure 6.28a and b. Figure 6.27b indicates that specimen FGC-2 lost about 5% of its load capacity at failure due to accelerated corrosion. However, its deflection capacity at failure was essentially not affected. Specimen FGC-3, on the other hand, lost 11% of its load capacity and 6% of its deflection capacity at failure. This specimen was subjected to accelerated corrosion for a longer period of time and lost a higher percentage of its internal steel reinforcement (compared to specimen FGC-2). By looking at the cracking patterns during structural testing in all specimens, it was noticed that the FGC specimens had about twice the number of load-induced cracks as the OPCC specimens (compare Figure 6.28a and c). This may be attributed to the strain-hardening and multiple-cracking behavior of the DFRCC material used in the FGC specimens. However, no sign of delamination of the concrete cover or between the concrete and the DFRCC layer was observed in the FGC specimens during structural testing. Although the loss of a steel section can still take place, particularly when the corrosion is induced, the damage to the steel/DFRCC material interfacial bond is probably quite low due to a potentially high tensile strain capacity of the DFRCC material. Moreover, the fibers in the DFRCC material can effectively bridge the cracks, thus improving the confining and holding capacity of the surrounding DFRCC material to the steel bar, resulting in minimum loss of bond due to corrosion. This may explain why the FGC specimens have retained most of their original deflection capacity despite undergoing accelerated corrosion. The scenario is quite different in the case of a corroded ordinary concrete beam. The damage of the bond between the concrete and steel rebar in a corroded RC beam is believed to contribute to the higher percentage of loss of load carrying and deflection capacities. It is argued that during corrosion, the expansive corrosion products caused cracking and damage to the cover concrete due to the brittle nature and low tensile strain capacity of ordinary concrete, which ultimately damaged the bond between the cover concrete and steel rebar in the corroded RC beam.

In the study by Sahmaran et al. (2005), the corroded beams were tested under four-point bending to determine their residual load–deflection curves and ultimate flexural loads after inducing the beams at different degrees of accelerated corrosion. The ECC beams show a substantially higher ultimate flexural load in comparison with that of the mortar beams. ECC specimens showed multiple-cracking behaviors with small crack spacing and tight crack widths (<0.1 mm). Figure 6.29a shows that the effect of accelerated corrosion has a marked influence on the load–deflection curves of mortar specimens. The ultimate load capacity decreases sharply with an increasing accelerated corrosion period. The typical load–deflection curves of ECC specimens after accelerated corrosion shown in Figure 6.29b reveal that the influence of accelerated corrosion test up to 50 h on the load–deflection curves of the ECC specimen is fairly small. Beyond 50 h of

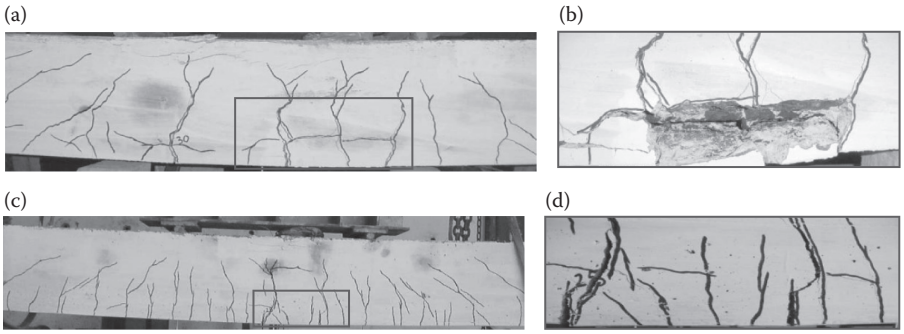

FIGURE 6.28 Typical cracking patterns of corroded beams: (a) OPCC-2 at about peak load; (b) close-up of region highlighted in (a) after failure; (c) FGC-3 at about peak load; and (d) close-up of region highlighted in (c) after failure. (From Maalej, M. et al., *Journal of Advanced Concrete Technology*, 1(3): 307–316, 2003. With permission from JCI.)

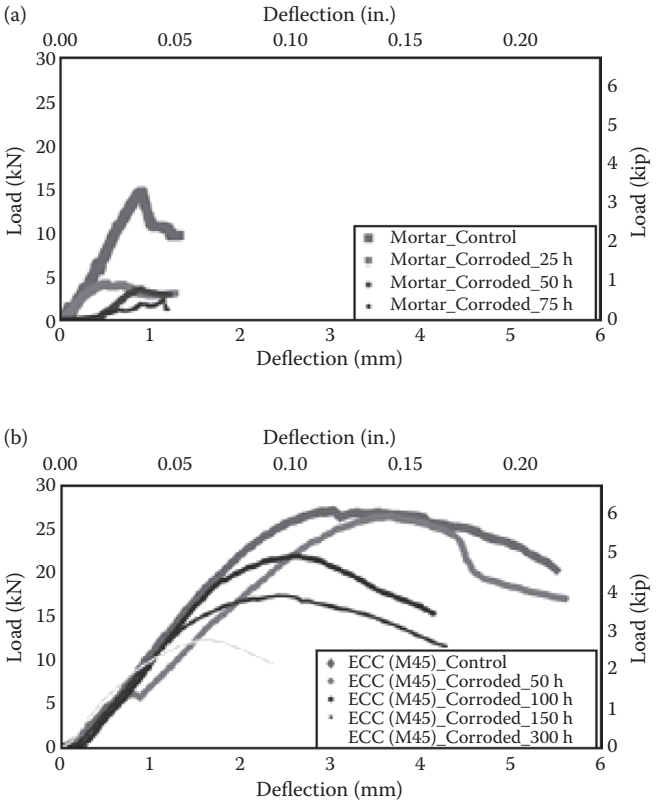

FIGURE 6.29 Load–deflection response of corroded and uncorroded (a) R/mortar and (b) R/ECC beams. (From Maalej, M. et al., *Journal of Advanced Concrete Technology*, 1(3): 307–316, 2003. With permission from JCI.)

accelerated corrosion, the ultimate residual flexural load capacity of ECC specimens decreased slowly as corrosion progressed.

Within the limited durability studies, the HPFRCC exhibited superior durability properties compared to the ordinary concrete, which warrants its potential application in RC structures for enhanced corrosion durability. However, lots of research still needs to be done on all aspects of its durability to confirm its full potential. In reality, however, RC structures under mechanical loads are often subjected to environmental influences. Since the crack width may be closed after unloading, a permeability test needs to be done under sustained loads, particularly under the strain-hardening stage in HPFRCC. HPFRCC is often made with cement-rich mix proportions, and shrinkage cracking easily occurs at the early stages. Shrinkage cracking may have some different geometry from that under mechanical loading. Although in the restrained shrinkage tests, the crack widths of this material were found to be small enough to resist the permeation of aggressive substances, permeability of damaged HPFRCC due to shrinkage cracking should also be studied. While HPFRCC showed superior protection of steel against corrosion in RC, only one study evaluated its potential against corrosion-induced cracking and particularly against spalling/delamination of cover concrete in the RC beams. In the study by Maalej et al. (2003), resistance of HPFRCC against spalling/delamination of cover concrete was evaluated only under 10% calculated steel loss. (Note that the actual steel loss in the beam was much less than the calculated value.) Therefore, the resistance of HPFRCC against spalling/delamination of cover concrete under heavily corroded reinforcing bars in RC beams needs to be evaluated to confirm its potential. While in the preliminary study, self-healing is observed in HPFRCC, more detailed studies need to be conducted to confirm this phenomenon and its effect on the permeability and corrosion.

6.4 CONCLUSIONS

Within the limited durability studies, HPFRCC exhibited superior corrosion durability properties compared to ordinary concrete, and this warrants its potential application in RC structures for enhanced durability against corrosion. The following conclusions can be drawn for the corrosion durability of HPFRCC based on the limited studies reviewed in this paper:

1. Due to the strain-hardening behavior of HPFRCC, the cracks thus formed are often under 100 μm in width, which warrants its superior permeability characteristics.
2. Due to its small crack width properties, the water and chloride permeability of cracked HPFRCC are comparable to those in the uncracked state.
3. The penetrations of chlorides in the cracked HPFRCC specimens are found to be several times lower than that of cracked OPC concrete.
4. Due to the above-mentioned improved impermeability characteristics of HPFRCC, the superior corrosion resistance of steel reinforcement in the cracked HPFRCC specimens is observed in terms of lower steel loss, slower rate of corrosion, and longer time required to achieve the same level of steel loss compared to an OPC specimen.
5. Superior corrosion-induced damage resistance of HPFRCC is also evident in terms of negligible to no corrosion-induced cracks and their small width.
6. The corroded HPFRCC specimens also exhibited better load–deflection behavior in terms of higher residual ultimate load and higher residual deflection at failure than its counterpart corroded OPC specimen.

REFERENCES

Ahmed, S.F.U., Maalej, M. and Paramasivam, P. (2006). Flexural responses of hybrid steel–polyethylene fibre reinforced cement composites containing high volume fly ash. *Journal of Construction and Building Materials*, 21: 1088–1097.

Ahmed, S.F.U., Maalej, M. and Paramasivam, P. (2007). Analytical model for tensile strain hardening and multiple cracking behaviour of hybrid fibre engineered cementitious composites. *ASCE, Journal of Materials in Civil Engineering*, 19(7): 527–539.

Ahmed, S.F.U. and Mihashi, H. (2007). A review on durability properties of strain hardening fibre reinforced cementitious composites (SHFRCC). *Journal of Cement and Concrete Composites*, 29(5): 365–376.

Ahmed, S.F.U. and Mihashi, H. (2010). Corrosion durability of strain hardening fiber reinforced cementitious composites. *Australian Journal of Civil Engineering*, 8(1): 13–25.

Edvardsen, C. (1999). Water permeability and autogenous healing of cracks in concrete, *ACI Materials Journal*, 4: 448–454.

Fisher, G. and Li, V. (2007). Effect of fiber reinforcement on the response of structural members. *Engineering Fracture Mechanics*, 74: 258–272.

Homma, D., Mihashi, H. and Nishiwaki, T. (2009). Self-healing capability of fiber reinforced cementitious composites. *Journal of Advanced Concrete Technology*, 7(2): 217–228.

JCI-DFRCC Committee. (2003). Technical report on the terminology. *Journal of Advanced Concrete Technology*, 1(3): 335–340.

Kan, L.L., Shi, H.S., Sakulich, A.R. and Li, V.C. (2010). Self-healing characterization of engineered cementitious composite materials. *ACI Materials Journal*, 107(6): 617–624.

Kawamata, A., Mihashi, H. and Fukuyama, H. (2002). Material design of hybrid fibre reinforced cementitious composites. *Journal of Advanced Concrete Technology*, 1(3): 283–290.

Kobayashi, K., Lizuka, T., Kurachi, H. and Rokugo, K. (2010). Corrosion protection performance of high performance fiber reinforced cement composites as a repair material. *Cement and Concrete Composites*, 32: 411–420.

Koda, M., Mihashi, M., Nishiwaki, T., Kikuta, T. and Kwon, S.M. (2011). Self-healing capability of fiber reinforced cementitious composites. *Proceedings of the International Workshop on Advances in Construction Materials Through Science and Technology*, Hong Kong, RILEM Proceedings Pro 79.

Lepech, M. and Li, V.C. (2005). Durability and long term performance of engineered cementitious composites. *Proceedings of the International Workshop on HPFRCC in Structural Applications*, Honolulu, Hawaii, May 23–26, 2005.

Li, M. and Li, V.C. (2011). Cracking and healing of engineered cementitious composites under chloride environment. *ACI Materials Journal*, 108(3): 333–340.

Li, V.C. (1992). Post-crack scaling relations for fibre reinforced cementitious composites. *Journal of Materials in Civil Engineering, ASCE*, 1.4(1): 41–57.

Li, V.C. and Leung, C.K. (1992). Steady state and multiple cracking of short random fibre composites. *Journal of Engineering Mechanics, ASCE*, 118(18): 2247–2264.

Li, V.C., Wang, S. and Wu, C. (2001). Tensile strain-hardening behaviour of polyvinyl alcohol engineered cementitious composites (PVA-ECC). *ACI Materials Journal*, 98(6): 483–492.

Li, V.C. and Wu, H.C. (1992). Conditions for pseudo strain-hardening in fibre reinforced brittle matrix composites. *Applied Mechanics Review*, 45(8): 390–398.

Maalej, M., Ahmed, S.F.U. and Paramasivam, P. (2003). Corrosion durability and structural response of functionally-graded concrete beams. *Journal of Advanced Concrete Technology*, 1(3): 307–316.

Maalej, M. and Li, V.C. (1995). Introduction of strain-hardening engineered cementitious composites in design of reinforced concrete flexural members for improved durability. *ACI Structural Journal*, 92(2): 167–176.

Martinola, G., Bauml, M.F. and Wittmann, F.H. (2002). Modified ECC applied as an effective chloride barrier. *Proceedings of the JCI International Workshop on Ductile Fibre Reinforced Cementitious Composites (DFRCC)—Application and Evaluation* (DRFCC-2002), Takayama, Japan, October 2002, pp. 171–180.

Mihashi, H., Ahmed, S.F.U. and Kobayakawa, A. (2011a). Corrosion of reinforcing steel in fiber reinforced cementitious composites. *Journal of Advanced Concrete Technology*, 9(2): 159–167.

Mihashi, H., Ahmed, S.F.U. and Kobayakawa, A. (2011b). Influence of crack widths on corrosion of reinforcing steel in fiber reinforced cementitious composites. *Proceedings of the International Workshop on Advances in Construction Materials Through Science and Technology*, Hong Kong, RILEM Proceedings Pro 79.

Miyazato, S. and Hiraishi, Y. (2005). Transport properties and steel corrosion in ductile fibre reinforced cement composites. *Proceedings of ICF*, Torino, Italy.

Naaman, A.E. and Reinhardt, H.W. (2006). Proposed classification of HPFRC composites on their tensile response. *Materials and Structures*, 39: 547–555.

Ogawa, A., Hitomi, Y. and Hoshiro, H. (2005). PVA-fibre reinforced high performance cement board. *Proceedings of the International Workshop on HPFRCC in Structural Applications*, Honolulu, Hawaii, May 23–26, 2005.

Qian, S., Zhou, J., Rooij, M.R., Schlangen, E., Ye, G. and Breugel, K.V. (2009). Self-healing behaviour of strain hardening cementitious composites incorporating local waste materials. *Cement and Concrete Composites*, 31: 613–621.

Sahmaran, M., Li, V.C. and Andrade, C. (2008). Corrosion resistance performance of steel reinforced engineered cementitious composite beams. *ACI Materials Journal*, 105(3): 243–250.

Yang, Y., Lepech, M.D., Yang, E.H. and Li, V.C. (2009). Autogenous healing of engineered cementitious composites under wet–dry cycles. *Cement and Concrete Research*, 39: 382–390.